

# On the Fracture Toughness of Polycrystalline Alumina Measured by SEPB Method

Toshihiko Nishida, Takeshi Shiono & Tomozo Nishikawa

Kyoto Institute of Technology, Faculty of Engineering and Design, Matsugasaki, Sakyo-ku, Kyoto 606, Japan

## Abstract

Fracture toughness ( $K_{IC}$ ) of a polycrystalline alumina was evaluated using a single edge precracked beam (SEPB) method. A Knoop indentation-induced microcrack was introduced into a bend bar specimen, and then a sharp pop-in precrack was developed by applying the bridge loading technique. The precrack length ( $a/W$ ) was varied by changing the indentation load and/or the support groove width of the anvil. The precracked specimens were fractured by three-point bending under a cross-head speed of 0.5 mm/min at room temperature.  $K_{IC}$  values of a polycrystalline alumina were dependent on precrack length for  $a/W < 0.35$ . The dependence was discussed in terms of residual stress around the indentation-induced crack and crack mouth opening displacement (CMOD).

Die Bruchzähigkeit ( $K_{IC}$ ) von polykristallinem Aluminiumoxid wurde durch Messungen an Biegebalcken mit scharfen künstlichen Anrissen (SEPB-Methode) bestimmt. Diese künstlichen Anrisse wurden mittels Knoop-Härteeindrücken erzeugt. Der Knoop-Härteeindruck wurde mit Hilfe der Brückentechnik erweitert. Die Anrißlänge ( $a/W$ ) wurde durch unterschiedliche Eindrucklasten und/oder durch die Änderung der Brückenparameter variiert. Diese angerissenen Biegeproben wurden anschließend unter drei-Punktbiegebeanspruchung mit einer Querschnittsgeschwindigkeit von 0.5 mm/min bei Raumtemperatur gebrochen. Die  $K_{IC}$ -Werte des polykristallinen Aluminiumoxids erwiesen sich als von der Anrißlänge abhängig, wenn das Verhältnis  $a/W < 0.35$  war. Diese Abhängigkeit wird in Zusammenhang mit den durch Härteeindruck hervorgerufenen Eigenspannungen und der Rißöffnungsverschiebung (CMOD) diskutiert.

On a évalué la ténacité ( $K_{IC}$ ) d'une alumine polycristalline par la méthode de l'entaille à arête simple

(SEPB). Une microfissure induite par empreinte Knoop a été introduite dans une éprouvette de flexion, puis une entaille nette a été développée in-situ en appliquant la technique de charge de pont. On a fait varier la longueur de l'entaille ( $a/W$ ) en changeant la charge appliquée et/ou la largeur de la rainure du support. Les échantillons entaillés ont été rompus en flexion trois points à une vitesse de 0.5 mm/min et à température ambiante. Les valeurs de  $K_{IC}$  d'une alumine polycristalline dépendent de la longueur de l'entaille lorsque  $a/W < 0.35$ . On discute cette dépendance en termes de contraintes résiduelles au voisinage de la fissure induite par l'empreinte et de déplacement de la fissure par ouverture du front (CMOD).

## 1 Introduction

In order to evaluate  $K_{IC}$  values of brittle ceramics, several experimental techniques have been proposed. A single edge precracked beam (SEPB) method has been recognized as one of the useful techniques, as it has advantages such as (a) simple, small and inexpensive test specimens, (b) a sharp, straight-through crack, (c) excellent reproducibility of  $K_{IC}$  value, and (d) easy application to high-temperature and hostile environments because of the simple bending mode.<sup>1,2</sup>

In the SEPB method, an indentation-induced microcrack or a sawed notch is usually introduced on a specimen surface as the starter of a pop-in precrack. It is well known that an indentation crack is more useful, since it results in the lower and reproducible pop-in load required.<sup>3</sup> It is reported, however, that  $K_{IC}$  values obtained by the SEPB method with an indentation as starter often depend on the indentation load and pop-in crack length.<sup>3,4</sup> The present work demonstrates experimentally the

effect of precracking conditions on  $K_{IC}$  values for a polycrystalline  $\alpha$ -alumina.

## 2 Experimental

The test material was normally sintered polycrystalline  $\alpha$ -alumina provided by Nippon Kagaku-Togyo Co. Ltd, Japan. It had a wide distribution of grain size, ranging from a few  $\mu\text{m}$  to 30  $\mu\text{m}$ , and the average value was 8.6  $\mu\text{m}$ . Its  $\text{Al}_2\text{O}_3$  content was 99.5% and small amounts of  $\text{SiO}_2$ ,  $\text{MgO}$  and  $\text{CaO}$  were added as sintering agents. Rectangular bars with dimensions of  $3 \times 4 \times 20$  mm were machined from a large block of the material for  $K_{IC}$  testing. All faces were ground in a lengthwise direction to 0.8  $\mu\text{m}$  in roughness. The edges were bevelled to eliminate undesirable microflaws.

A Knoop indentation-induced microcrack was introduced into the center of a specimen surface, and then a sharp single edge pop-in precrack was developed by applying the bridge indentation technique as shown in Fig. 1. The specimen width ( $W$ ) and crack length ( $a$ ) are demonstrated in the figure. The relative pop-in precrack length ( $a/W$ ) was varied by changing the indentation load (20, 30, 50 kgf) and/or the width of the support groove (4, 5, 6 mm). A dye-penetration technique was adopted for easy measurement of the precrack length.

The single edge precracked beam (SEPB) specimens were fractured by the three-point bend configuration using the span of 16 mm under a cross-head speed of 0.5 mm/min at room temperature in air.

For the calculation of  $K_{IC}$  value, the equation given in ASTM<sup>5</sup> was used, because the support span ( $S$ ) was designated to be four times as long as the specimen width ( $W$ ). The equation is expressed as follows:

$$K_{IC} = \frac{P_f S}{BW^{1.5}} f(a/W)$$

$$f(a/W) = \frac{3(a/W)^{1/2} [1.99 - (a/W) \times (1 - a/W)(2.15 - 3.93a/W + 2.7a^2/W^2)]}{2(1 + 2a/W)(1 - a/W)^{3/2}} \quad (1)$$

where  $P_f$  and  $B$  are the maximum fracture load and the specimen thickness, respectively.

Problems accompanying preparation of SEPB specimens include the following difficulties: the inclination of the pop-in crack front (the pop-in crack front is not formed vertical to the direction of crack propagation), and the deflection of the precracked fracture surface (both the pop-in pre-

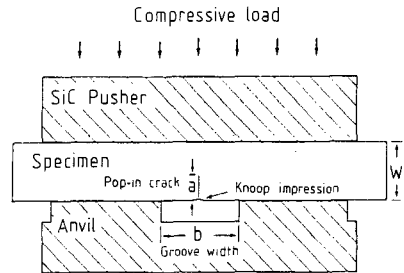


Fig. 1. Scheme of the technique for introducing sharp single edge precrack into a bend-bar specimen by bridge loading.

cracked plane and the fracture surface produced by the post-bending fracture test deflect from a plane perpendicular to a lengthwise direction of the specimen). Thus the test results are supposed to be only adopted when they satisfy the following two proposed conditions, since these difficulties may result in undesirable errors in the  $K_{IC}$  test. The precrack length is measured at three points which divide the front into four sections. The difference between the length at any two points is then required to be less than 10% of the average precrack length. The deflection of the fracture surface also must be less than 10% of the specimen width.

## 3 Results and Discussion

### 3.1 Effect of indentation load on $K_{IC}$

Table 1 shows  $K_{IC}$  of a polycrystalline alumina measured by different Knoop indentation loads. The obtained values seem to have no dependence on the indentation load. From a standpoint of relative precrack length ( $a/W$ ), however, the result can be divided into two parts, as shown in the table. In the case of shorter crack length,  $0.15 < a/W < 0.35$ , the dependence of  $K_{IC}$  on indentation load is clearly recognized. A similar tendency has already been

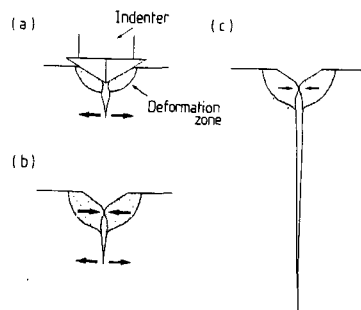


Fig. 2. Schematics of the residual stress effect of indentation-induced microcrack (a and b) and pop-in precrack (c).

**Table 1.** Effect of Knoop indentation load introduced as a starter pop-in precrack on  $K_{IC}$  measured by SEPB method for a polycrystalline alumina

Indentation load (kgf)	$K_{IC} (MPa m^{0.5})$		
	$0.15 < a/W < 0.80$	$0.15 < a/W < 0.35$	$0.35 < a/W < 0.80$
20	$4.88 \pm 0.32$	$4.53 \pm 0.15$	$5.03 \pm 0.16$
30	$4.66 \pm 0.32$	$4.39 \pm 0.15$	$4.92 \pm 0.19$
50	$4.71 \pm 0.47$	$4.17 \pm 0.03$	$5.03 \pm 0.35$

reported for polycrystalline silicon nitride<sup>4</sup> and silicon carbide<sup>6</sup> ceramics.

One of the reasons would be the effect of residual compressive stress around the indentation impression introduced as a starter pop-in precrack. The residual stress has been well known to have crucial influence on  $K_{IC}$  measured by the controlled surface flaw (CSF) method.<sup>7</sup> Figure 2 shows a scheme of stress states when the indentation is introduced.<sup>8</sup> In a brittle material, the indentation not only produces a plastic indentation impression but also introduces semi-ellipse microcracks (median cracks) (Fig. 2(a)). Compressive stresses in the plastically deformed region persist after the indentation load is removed completely, resulting in tensile stresses at a tip of the microcrack as a counteraction (Fig. 2(b)). This tensile stress is expected to remain, to some extent, even after introducing pop-in precrack (Fig. 2(c)). If there is a proportional relationship between indentation load and residual stress, and it yields a sizable effect on the bending strength, the apparent  $K_{IC}$  must be lower for higher indentation load.

The other reason for the indentation load dependent  $K_{IC}$  may be the effect that  $K_{IC}$  values depend on pop-in precrack length. As already reported, the indentation load shows a reverse relationship to the precrack length.<sup>3</sup> The smaller the

microcrack as a starter pop-in precrack, the higher the pop-in load becomes, resulting in a longer pop-in precrack. Taking this into consideration, the tendency that longer precrack (i.e. lower indentation load) gives higher  $K_{IC}$ , shown in Table 1, is recognized as a behavior similar to the effect of rising  $R$ -curve.<sup>9</sup>

In order to clarify which reasons discussed above have a dominant influence on  $K_{IC}$ , obtained data was rearranged. The result (original data of Table 1) is given in Fig. 3 by plotting the relationship between  $P_f S/BW^{1.5}$  and  $f(a/W)^{-1}$ . The figure also gives the data of specimens the indented surfaces of which were ground and polished to a depth three or four times that of the indent depression to eliminate residual stresses around the impression, after developing a pop-in precrack from a Knoop indentation crack induced at a load of 20 kgf.

In the case of eliminating the residual stress the plot points are, to a large extent, satisfied with a linear relationship through the origin, and then  $K_{IC}$  of this polycrystalline alumina is determined as  $5.0 \text{ MPa m}^{0.5}$  from the slope, as shown in Fig. 3. This result strongly indicates that the dependence of  $K_{IC}$  on the indentation load in the present work does not stem from pop-in precrack length through its rising  $R$ -curve behavior, but mainly from the residual stress around the indentation impression. And the effect of the residual stress appears only in the case of shorter precrack length ( $a/W < 0.35$ ).

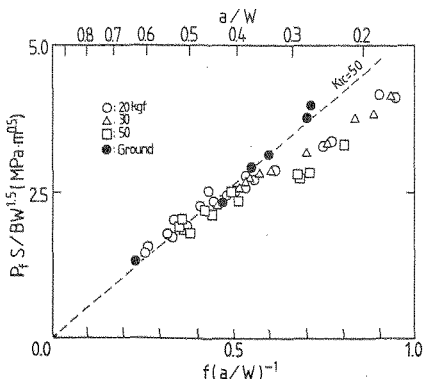


**Fig. 3.** Fracture load as a function of relative crack length for a polycrystalline alumina.

### 3.2 Residual stress around an indentation-induced crack

As shown in Fig. 2, the residual compressive stress produced by the micro-indenter on the surface of a ceramic is considered to be introduced by a plastic deformation that protrudes from both sides of fracture surfaces beneath the indentation impression so that the microcrack opens.<sup>8</sup> In order to identify this protrusion, the fracture surface beneath a Knoop impression was observed by scanning electron microscopy (SEM), as shown in Fig. 4. The observation shows that intergranular fracture characteristically developed perpendicular to the

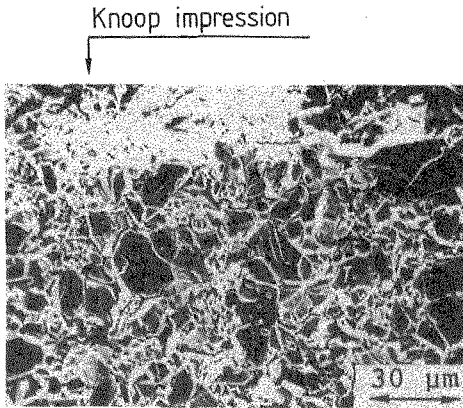


Fig. 4. SEM photograph of microcracks beneath a Knoop indentation impression for a polycrystalline alumina.

direction of indentation. In this polycrystalline alumina, the indentation-induced plastic zone contains some amount of dilatant volume change accompanied by microcracking, which may yield one of the reasons for the residual compressive stress.

For further examination of the residual compressive stress, crack mouth opening displacement (CMOD) of an indentation-induced microcrack was measured on the indented surface of ceramics. The crack develops along the major diagonal direction of the rhombo-shaped impression, and remains open a little as schematically shown in Fig. 5.

Assuming a simple proportional relationship, the crack mouth opening displacement at the center of the impression ( $\delta_1$ ) is approximated by eqn (2):

$$\delta_1 = \delta_2 \frac{l_1}{l_2} \quad (2)$$

where  $l_1$  is length from the center of the impression to the crack tip,  $l_2$  is length of the developed microcrack and  $\delta_2$  is crack width at the indentation edge. Table 2 shows  $\delta_1$  calculated with  $l_1$ ,  $l_2$  and  $\delta_2$  measured by SEM photographs. Taking the possibility of underestimation of  $\delta_2$  values into consideration because of the complexity of the state of the crack developing in the polycrystalline alumina, the protrusion which results in the residual stress may

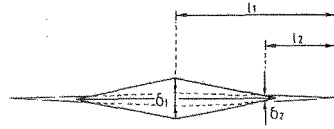


Fig. 5. A model for Knoop indentation-induced surface flaw on brittle ceramic surface.

open the mouth of a Knoop indentation-induced crack by a few  $\mu\text{m}$ .

### 3.3 Crack mouth opening displacement at the onset of fracture

Supposing specimens were perfectly linear elastic, CMOD at the onset of brittle fracture of SEPB specimen in bending is given by eqn (3):<sup>10</sup>

$$\delta_f = \frac{4\delta_r a}{E'} V(a/W)$$

$$V(a/W) = 0.76 - 2.28(a/W) + 3.87(a/W)^2 \quad (3)$$

$$- 2.04(a/W)^3 + \frac{0.66}{(1 - (a/W))^2}$$

where  $E'$  is elastic modulus. Equation (3) has been confirmed to be applicable to brittle ceramics such as glass and silicon nitride by experiments using a laser interferometric strain gage with high resolution.<sup>11</sup>

Figure 6 shows  $\delta_r$  of a polycrystalline alumina calculated by eqn (3), with  $E'$  of 380 GPa. The  $E'$  value was evaluated experimentally by the dynamic resonance technique. The effect of Poisson's ratio was neglected.  $\delta_r$  for the precrack lengths of

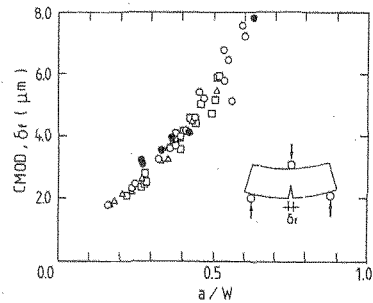


Fig. 6. Calculated CMOD at the onset of brittle fracture of SEPB specimen as a function of relative crack length for a polycrystalline alumina.

Table 2. Geometrical parameters of a Knoop impression and the induced crack shown in Fig. 5 for a polycrystalline alumina

Indentation load (kgf)	$l_1$ ( $\mu\text{m}$ )	$l_2$ ( $\mu\text{m}$ )	$\delta_1$ ( $\mu\text{m}$ )	$\delta_2$ ( $\mu\text{m}$ )
20	$316 \pm 8.5$	$112 \pm 9.8$	$0.49 \pm 0.11$	$0.17 \pm 0.03$
30	$423 \pm 6.8$	$156 \pm 8.3$	$0.83 \pm 0.14$	$0.31 \pm 0.04$
50	$534 \pm 32$	$142 \pm 33$	$1.45 \pm 0.25$	$0.37 \pm 0.07$

$a/W < 0.35$  where the residual stress has been noted to have an effect on the  $K_{IC}$  of less than  $4 \mu\text{m}$ . As discussed in Section 3.2, the residual stress beneath the indentation impression has a critical influence on  $K_{IC}$  before the CMOD becomes a few  $\mu\text{m}$ . This value is approximately equal to  $\delta_f$  calculated above. In the polycrystalline alumina studied in the present work, the effect of residual stress on  $K_{IC}$  in SEPB test appears in the region of short pop-in precrack lengths of  $a/W < 0.35$  because of a small CMOD at the failure point.

#### 4 Summary

It has often been remarked that  $K_{IC}$  values in the SEPB test depend on the indentation load which introduces a surface microflow as a starter of pop-in precracking. In order to clarify the dependence, the residual stress around a Knoop indentation and the CMOD at incipient brittle fracture of SEPB specimen for a polycrystalline alumina were examined. It is emphasized that the test conditions such as specimen size, pop-in precrack length, indentation load, etc., for  $K_{IC}$  measurement in the

SEPB method must be chosen to avoid uncertainties by the residual stresses introduced by indentation.

#### Acknowledgement

The authors would like to thank Mr A. Nagai for assistance in performing the experiments.

#### References

1. Sadahiro, T., *Powder and Powder Metallurgy*, **33** (1986) 422-5.
2. Nose, T. & Fujii, T., *J. Am. Ceram. Soc.*, **71** (1988) 328-33.
3. Nishida, T., Shiono, T., Nagai, A. & Nishikawa, T., *J. Ceram. Soc. Japan*, **96** (1988) 608-12.
4. Murayama, N., Sakaguchi, S. & Wakai, F., *J. Ceram. Soc. Japan*, **95** (1987) 1034-6.
5. ASTM STP E399-83 Annual ASTM Standards, 1983, p. 492.
6. Nishida, T., Shiono, T., Nagai, A. & Nishikawa, T., *Powder and Powder Metallurgy*, **36** (1989) 141-3.
7. Petrovic, J. J., Jacobson, L. A., Talty, P. K. & Vasudevan, K., *J. Am. Ceram. Soc.*, **58** (1975) 113-16.
8. Petrovic, J. J., Dirks, R. A., Jacobson, L. A. & Mendiratta, M. G., *J. Am. Ceram. Soc.*, **59** (1976) 177-8.
9. Freiman, S. W., *Am. Ceram. Soc. Bull.*, **67** (1988) 392-402.
10. Okamura, H., *Introduction to Linear Fracture Mechanics*. Baifukan Co., Tokyo 1976, p. 218, in Japanese.
11. Jenkins, M. G., Kobayashi, A. S., Sakai, M., White, K. W. & Bradt, R. C., *Am. Ceram. Soc. Bull.*, **66** (1987) 1734-8.